Robotica (2022), **40**, pp. 154–169
doi:10.1017/S0263574721000448

CAMBRIDGE
UNIVERSITY PRESS

RESEARCH ARTICLE

Research on mechanical optimization methods of cable-driven lower limb rehabilitation robot

Yan-lin Wang, Ke-yi Wang*, Yu-jia Chai, Zong-jun Mo, and Kui-cheng Wang

College of Mechanical and Electrical Engineering, Harbin Engineering University, Harbin 150001, China
*Corresponding author. Email: wangkeyi@hrbeu.edu.cn

Received: 11 December 2020; **Revised:** 27 March 2021; **Accepted:** 29 March 2021; **First published online:** 7 May 2021

Keywords: Cable-driven robot, Rehabilitation robot, Mechanical characteristics, Optimization algorithms, Quality of feasible workspace

Abstract

In order to improve the working performance of the lower limb rehabilitation robot and the safety of the trained object, the mechanical characteristics of a cable-driven lower limb rehabilitation robot (CDLR) are studied. The dynamic model of the designed CDLR was established. Four kinds of cable tension optimization algorithms were proposed to obtain a good rehabilitation training effect, and the quality of the feasible workspace of the CDLR was analyzed. Finally, a real-time evaluation index of the cable tension optimization algorithms was given to measure the calculation speed of the optimization algorithms. The numerical research results were provided to confirm the characteristics of the four kinds of the optimization algorithms. The research results provide a basis for the follow-up research on the safety and compliance control strategy of the CDLR system.

1. Introduction

The global aging population has been increasing [1], and there is a high incidence of stroke, hemiplegia, and hemiplegia in the aging population [2, 3]. In addition, there are other reasons (e.g., natural disasters, traffic accidents, etc.) that have caused the number of patients with limb movement disorders to increase. The exercise ability of patients can be enhanced or the part of the exercise ability can be recovered through reasonable and scientific rehabilitation treatment and training. However, global medical resources are a serious shortage. Therefore, it is of practical significance to study the medical rehabilitation robots instead of rehabilitation therapists to improve the rehabilitation training effect of patients and reduce the work pressure of rehabilitation therapists [4, 5].

Rehabilitation robot is a comprehensive research achievement in multidisciplinary fields such as rehabilitation medicine, biomechanics, mechanics, and control science, and so on. It is a very complex human–machine coupling system, which is also a study frontier and hot topic in the robotics field [6, 7]. According to the structural characteristics of limb rehabilitation robots, the studied limb rehabilitation robots can be divided into two categories: exoskeleton type and end traction type limb rehabilitation robots. They have their advantages. For example, exoskeleton rehabilitation robots have strong training targets, and the joints of exoskeleton rehabilitation robots and the joints of human limbs have a strict correspondence relationship. Exoskeleton rehabilitation robots can complete independent control training of single joint and comprehensive control training of multiple joints. Typical applications include a 7-DOF cable-driven arm exoskeleton (CAREX-7) studied by Beihang University [8], 6-DOF lower limb exoskeleton (LLE) studied by University Kebangsaan Malaysias [9, 10], lower limb wearable robotic exoskeleton (LLWRE) studied by University of Iceland [11], and so on. However, the exoskeleton rehabilitation robot has some problems such as complex structure, difficult control, poor

© The Author(s), 2021. Published by Cambridge University Press.

https://doi.org/10.1017/S0263574721000448 Published online by Cambridge University Press

man-machine compatibility, and so on [12, 13], The end traction type rehabilitation robots generally use cables instead of rigid links as the transmission elements of motion and force, which is called the cable-driven rehabilitation robots. This type of robots has some advantages such as small mass and inertia, high motion accuracy, strong reconstruction ability, good human–machine compatibility performance, adjustable system stiffness, and so on [14]. These performance characteristics make the cable-driven parallel robots have a good application in the rehabilitation medicine field. Zi et al. [15, 16] studied a cable-driven waist rehabilitation training robot. During the training process, the patient must stand on the moving platform, and the cables pull the moving platform to complete the waist training of patients. Carbone et al. [17] designed a novel cable-driven parallel robot for the assistance of patients in rehabilitation training of both upper and lower limbs. Barbosa et al. [18] designed a cable-driven lower limb rehabilitation robot, which is composed of a fixed base and a moving platform that can perform the individual movements training of the hip, the knee, and the ankle. Wang and Wang et al. [19, 20] designed a CDLR with a rigid motion branch. The movement of the rigid motion branch increases the effective workspace, maneuverability, and diversification of the training form of the rehabilitation robot.

Cable-driven rehabilitation robots have the abovementioned performance advantages, but the cable can only provide one-way restraint force to the trained object, and the flexibility of the cables reduces the system stiffness of the cable-driven rehabilitation robots, which not only increases the control difficult of the CDLR, but also reduces the stability and safety of the CDLR system. In order to improve the kinematic characteristics of cable-driven parallel robots, researchers have done a lot of work. For example, the stability [19, 21, 22] and safety [23] of cable-driven rehabilitation robots were analyzed based on the characteristics of cable tension and system stiffness. Considering the workspace, cables tensions, cables sagging, compactness, singularity, and safety of the cable-driven parallel robot (CDPR), a dimensional synthesis optimization method [24] was proposed. But the safety index of the CDPR was defined with the minimum distance between the cables and the patient in the rehabilitation task [24]. It can only ensure that there is no interference between the patient and the robot, and cannot completely ensure the safety of patients in the rehabilitation training. The straight-line model and catenary model of the cable [25, 26] were established. The structure optimization of the robot [27] and the compound control strategy [28] were studied.

In order to evaluate the dynamical stability and safety of CDLR, the cable tension factors [5, 6, 23, 29] were defined to measure the ability of the system to resist external interference in different directions based on the distribution of cable tension. Due to the evaluation of the CDPR's performances cannot be performed using the performance indexes for parallel robots with rigid links, an improved wrench exertion capability index was proposed to evaluate the maximum tension force that cable can exert along a direction of interest. The improved wrench exertion capability formulation can be used to analyze any cable parallel robots [30, 31]. A kinematic optimization of the limb rehabilitation robot driven by pneumatic muscles was given by maximizing the mean value of the local transmission index subject to the lower and upper bounds of design variables based on the genetic algorithm [32]. However, due to the hysteresis of pneumatic muscles, the control of the mechanism is still facing a great challenge in practical application. In order to prevent the pseudo-drag phenomenon of cables and to ensure the safety of patients, the minimum tension force of cables must be limited [23, 33]. Therefore, in actual applications, the calibrated sensors and the data collected by them must be used to guarantee the existence of the minimum tension force in cables in rehabilitation training [33]. The solution method of the continuous cable tension [34] for a movable CDLR was obtained using the 2-norm optimization algorithm of the cable tension.

However, the cable tension optimization problem of the cable-driven parallel robots is the basis of the abovementioned problem. The distribution of cable tensions obtained by different optimization algorithms is different, which has practical significance for the stability of the system and the safety of the trained object in rehabilitation training. Therefore, the mechanical characteristics of the designed CDLR are studied in this paper, four kinds of cable tension optimization algorithms were proposed, and the

https://doi.org/10.1017/S0263574721000448 Published online by Cambridge University Press

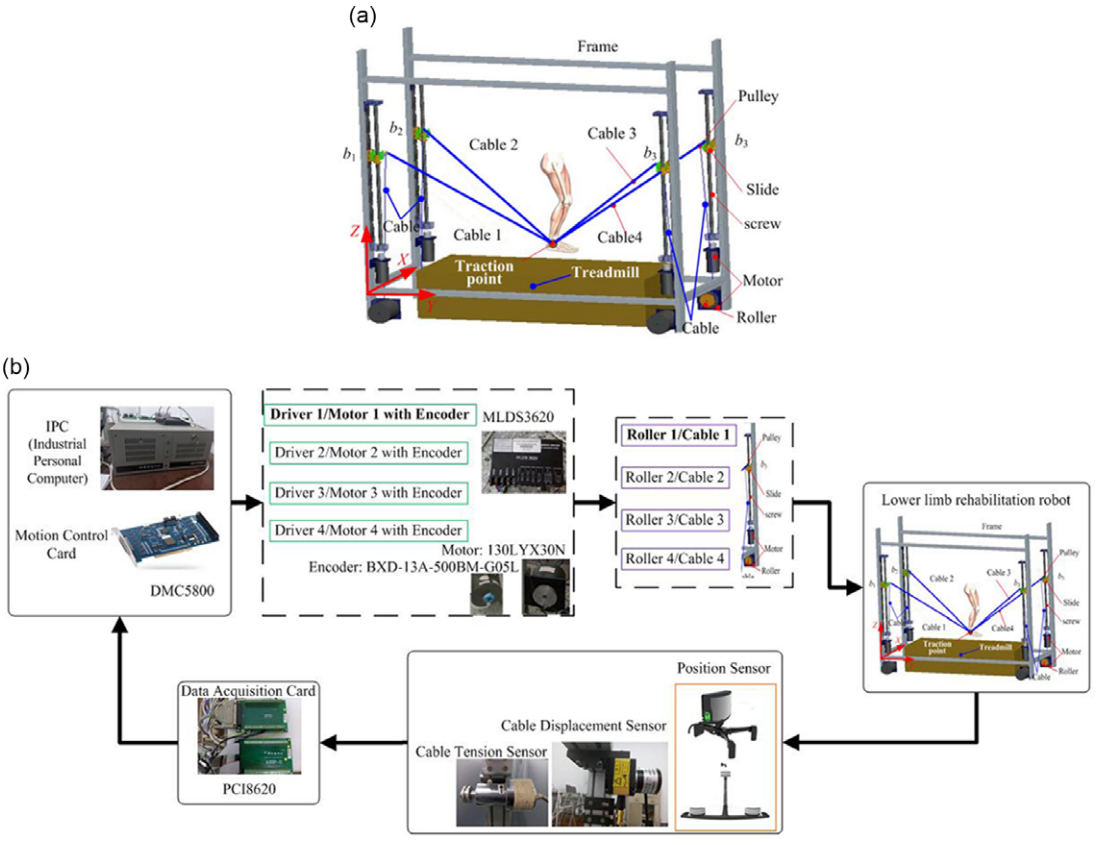


Figure 1. *Model of cable-driven lower limb rehabilitation robot. (a) Cable-driven lower limb rehabilitation robot. (b) Block diagram of configuration for the CDLR.*

quality of the feasible workspace obtained by different optimization algorithms was analyzed. In order to measure the calculation speed of four kinds of cable tension optimization algorithms, a real-time evaluation index for cable tension calculation was defined. Finally, the influences of the four kinds of cable tension optimization algorithms on the robot's feasible workspace and cable tensions were analyzed through one example. The research results lay the foundation for the safety evaluation and the control strategy of human–machine compliance for the CDLR.

2. CDLR

The structural model of the designed CDLR is shown in Fig. 1(a), which is mainly composed of cables, screw slider mechanisms, motors, pulleys, rollers, frame, and treadmill. One end of the cable is attached to the ankle joint of human lower limb, and the other end of the cable is attached to the roller through a pulley. The roller is driven by a torque motor to realize the movement control of the cable. The coordinated movement of four groups of cables can realize the rehabilitation training of the lower limb. The height of pulleys can be adjusted by the screw slider mechanism to meet the needs of patients with different heights and different rehabilitation training tasks.

In rehabilitation training, according to the height of the trained object and the requirements of training tasks, the position of the slider in the screw slider mechanism can be adjusted by the motor. Of course, the slider movement can also be adjusted in real-time according to the needs of the planned training tasks

https://doi.org/10.1017/S0263574721000448 Published online by Cambridge University Press

in rehabilitation training. The tasks are planned according to the training needs of the trained objects, and the rehabilitation movement of the lower limbs is controlled by the coordinated movement of four groups of cables. The speed of the treadmill is controlled to achieve different intensities of rehabilitation training. In addition, gait training and running training in passive training mode, active training mode, and auxiliary training mode can be realized by reasonably setting the motor's movement mode, the height of the slider, and the movement speed of the treadmill, which increases the diversity of lower limb rehabilitation training forms.

The configuration of the designed CDLR is shown in Fig. 1(b), which is mainly composed of IPC, motion control card, drivers and motors with encoder, rollers, and cables, mechanism of the CDLR, sensors, and data acquisition card. IPC and motion control cards generate control signals according to training tasks and transmit them to drivers. The motors drive the cables to complete the coordinated movement of the lower limb traction point to realize the lower limb rehabilitation training. The position data of the traction point are collected via the position sensor. The cable tensions data are collected via cable tension sensors. The cable length data are collected via cable displacement sensors. These collected data are feedbacked to the IPC via the data acquisition card to realize closed-loop control of the CDLR system. The sensors system can monitor each cable's tension and realize efficient control of actuators to assure different rehabilitation programs for patients.

3. Mechanical analysis

3.1. Dynamics

In the global coordinate system *O-XYZ*, assume the position of pulley $b_i (i = 1, 2, 3, 4)$ is $b_i(x_i, y_i, z_i)$, the position of ankle joint P of the lower limb is $P(x, y, z)$, and the effective length of the cable is L_i, so the length vector of the cable can be expressed as

$$\boldsymbol{L}_i = \boldsymbol{Ob}_i - \boldsymbol{OP}. \tag{1}$$

The effective length of the cable can be written as

$$L_i = \frac{\boldsymbol{L}_i}{\|\boldsymbol{L}_i\|} = \sqrt{(\boldsymbol{Ob}_i - \boldsymbol{OP})^T(\boldsymbol{Ob}_i - \boldsymbol{OP})}. \tag{2}$$

Rehabilitation training of lower limbs is realized through the coordinated motion control of four group cables. The mechanical balance equation of the CDLR can be expressed as

$$\boldsymbol{J}^T\boldsymbol{T} = \boldsymbol{F}, \tag{3}$$

where $\boldsymbol{T} = [\, t_1 \; t_2 \; t_3 \; t_4 \,]^T$ is the cable tensions vector. In order to prevent the pseudo-drag phenomenon of cables and ensure the safety of trained objects, the cable tension should meet the conditions: $\boldsymbol{T}_{\min} = [\, t_{1,\min} \; t_{2,\min} \; t_{3,\min} \; t_{4,\min} \,]^T \le \boldsymbol{T} \le \boldsymbol{T}_{\max} = [\, t_{1,\max} \; t_{2,\max} \; t_{3,\max} \; t_{4,\max} \,]^T$. $\boldsymbol{T}_{\min}$ and $\boldsymbol{T}_{\max}$ are pre-tension forces and maximum allowable tension forces. $\boldsymbol{F}$ is the external force wrench acting on the traction point of the lower limbs (including the force of the lower limbs and the gravity of the traction point equipment). The structure matrix $\boldsymbol{J}^T$ of the CDLR can be expressed as

$$\boldsymbol{J}^T = \begin{bmatrix} \boldsymbol{J}_1 & \boldsymbol{J}_2 & \boldsymbol{J}_3 & \boldsymbol{J}_4 \end{bmatrix}. \tag{4}$$

According to the wrench closure principle, the designed CDLR satisfies the wrench closure conditions. But the structural matrix is not a square matrix, the cable tensions need to be calculated by the generalized inverse of the structure matrix. The cable tensions can be expressed as

$$\boldsymbol{T} = \boldsymbol{T}_s + \boldsymbol{T}_n = \boldsymbol{J}^+\boldsymbol{F} + \lambda \cdot \boldsymbol{N}\left(\boldsymbol{J}^T\right), \tag{5}$$

where $\boldsymbol{J}^+ = \boldsymbol{J}^T(\boldsymbol{J}\boldsymbol{J}^T)^{-1}$ is the generalized inverse of the structure matrix $\boldsymbol{J}^T \cdot \lambda$ is an arbitrary vector. $\boldsymbol{N}(\boldsymbol{J}^T)$ is the null space vector of the structure matrix $\boldsymbol{J}^T$, and the ith element is $\boldsymbol{N}_i(\boldsymbol{J}^T) = (-1)^{-i+1} \cdot \det[\boldsymbol{J}_1 \cdots \boldsymbol{J}_{i-1} \; \boldsymbol{J}_{i+1} \; \cdots \; \boldsymbol{J}_m]$. $\boldsymbol{T}_s = [\, t_{s,1} \; t_{s,2} \; t_{s,3} \; t_{s,4} \,]^T$ is the only special solution to the mechanical equilibrium Eq. (3). T_n is the general solution term to the balance Eq. (3), and this term does not do

https://doi.org/10.1017/S0263574721000448 Published online by Cambridge University Press

work to the system. But it can change the distribution of the cable tensions in the system, so it can be called the internal force of the system. Since the CDLR studied in this paper is a fully constrained positioning mechanism, λ is an arbitrary scalar.

Based on the above discussion, the range of the value λ is

$$\lambda_l \le \lambda \le \lambda_h, \tag{6}$$

where the lower bound λ_l and upper bound λ_h of the value λ are as follows:

$$\begin{cases} \lambda_l = \max\limits_{1\le i\le 4}\left\{\min\limits_{1\le i\le 4}\left(\dfrac{t_{i,\min}-t_{s,i}}{\boldsymbol{N}_i(\boldsymbol{J}^T)}, \dfrac{t_{i,\max}-t_{s,i}}{\boldsymbol{N}_i(\boldsymbol{J}^T)}\right)\right\} \\ \lambda_h = \min\limits_{1\le i\le 4}\left\{\max\limits_{1\le i\le 4}\left(\dfrac{t_{i,\min}-t_{s,i}}{\boldsymbol{N}_i(\boldsymbol{J}^T)}, \dfrac{t_{i,\max}-t_{s,i}}{\boldsymbol{N}_i(\boldsymbol{J}^T)}\right)\right\} \end{cases}. \tag{7}$$

If the convex combination formed by λ_l and λ_h is expressed as λ^c, the feasible solution of cable tensions can be expressed as

$$\boldsymbol{T} = \boldsymbol{J}^{+}\boldsymbol{F} + \lambda^c \cdot \boldsymbol{N}(\boldsymbol{J}^T). \tag{8}$$

3.2. Cable tension optimization algorithms

Equation (6) is a linear constraint condition about λ. According to Eq. (8), the choice arbitrariness of λ will cause the nonunique and uncertainty of the general solution $\boldsymbol{T}_n$ of cable tensions. Therefore, the distribution of cable tensions should be adjusted and optimized by adjusting the value λ. The optimization problem of the cable tensions of the CDLR can be transformed into a single-objective optimization problem about λ under the system constraints. The optimization model can be described as

$$\begin{cases} \min f(\lambda) \\ s.t.\ \boldsymbol{J}^T\boldsymbol{T} = \boldsymbol{F} \\ \quad \lambda_l \le \lambda \le \lambda_h \end{cases}, \tag{9}$$

where $f(\lambda)$ is the optimization objective function of the cable tensions, which is a polynomial about λ. When choosing different optimization objective functions, the cable tension optimization model (9) has different physical meanings [35]. The commonly used cable tension optimization objective function is the minimum *p*-norm of the cable tension. Equation (6) is a linear constraint condition about λ. When the optimization objective function is the minimum *p*-norm of the cable tension, the optimization objective function is a convex function, in which the feasible region is also a convex set. For the CDLR studied in this paper, the feasible region is a one-dimensional array. Therefore, the optimization objective function $f(\lambda)$ is continuous and steerable in $[\lambda_l, \lambda_h]$. According to the optimization theory, the feasible solution of the optimized cable tension is the global optimal and only solution [29].

In order to meet the requirements of rehabilitation training and real-time calculation of the CDLR, four kinds of algorithms suitable for cable tension optimization are proposed as the optimization objective function in this paper: minimum 2-norm optimization algorithm, minimum 3-norm optimization algorithm, minimum variance optimization algorithm, and CF(Closed-form) optimization algorithm.

3.2.1. Minimum 2-norm optimization algorithm

The minimum 2-norm optimization algorithm of cable tensions is the most commonly used optimization method. This algorithm is a quadratic programming algorithm, and the solved cable tensions are continuous. The minimum 2-norm optimization objective function $f(\lambda)$ of cable tensions can be expressed as

$$f(\lambda) = \min\left(\sqrt{t_1^2 + t_2^2 + t_3^2 + t_4^2}\right). \tag{10}$$

https://doi.org/10.1017/S0263574721000448 Published online by Cambridge University Press

Let,

$$\begin{cases} f = \left(t_1^2 + t_2^2 + t_3^2 + t_4^2\right) = \sum_{i=1}^{4} \left(t_{s,i} + n_i\lambda\right)^2 = A\lambda^2 + B\lambda + C \\ A = n_1^2 + n_2^2 + n_3^2 + n_4^2 \\ B = 2\left(t_{s,1}n_1 + t_{s,2}n_2 + t_{s,3}n_3 + t_{s,4}n_4\right) \\ C = t_{s,1}^2 + t_{s,2}^2 + t_{s,3}^2 + t_{s,4}^2 \end{cases}, \tag{11}$$

where n_i is the element in the null space vector of the structure matrix J^T.

There is $\frac{\partial f}{\partial \lambda} = 2A\lambda + B$, and let $\frac{\partial f}{\partial \lambda} = 0$, so

$$\lambda = -\frac{B}{2A} = \frac{t_{s,1}n_1 + t_{s,2}n_2 + t_{s,3}n_3 + t_{s,4}n_4}{n_1^2 + n_2^2 + n_3^2 + n_4^2}. \tag{12}$$

There are three situations at this time:

(a) When $\lambda_l \le \lambda \le \lambda_h$, λ^c can be expressed as

$$\lambda^c = -\frac{B}{2A} = \frac{t_{s,1}n_1 + t_{s,2}n_2 + t_{s,3}n_3 + t_{s,4}n_4}{n_1^2 + n_2^2 + n_3^2 + n_4^2}, \tag{13}$$

B in Eq. (11) can be further organized as

$$B = 2\boldsymbol{F}(\boldsymbol{J}\boldsymbol{J}^T)^{-1}\boldsymbol{J} \cdot \boldsymbol{N}_i\left(\boldsymbol{J}^T\right). \tag{14}$$

Due to $\boldsymbol{J} \cdot \boldsymbol{N}_i(\boldsymbol{J}^T) = \begin{bmatrix} 0 & 0 & 0 \end{bmatrix}^T$, $B = 0$, which means that $\lambda^c = 0$. So the cable tensions $\boldsymbol{T} = \boldsymbol{T}_s$.

(b) When $\lambda < \lambda_l$, let $\lambda^c = \lambda_l$. The cable tensions can be written as

$$\boldsymbol{T} = \boldsymbol{T}_s + \lambda^c \cdot \boldsymbol{N}\left(\boldsymbol{J}^T\right) = \boldsymbol{T}_{\min}. \tag{15}$$

That is, the cable tension is smaller than the minimum pre-tension force, and the cable tension will be corrected to the minimum cable tension at this time.

(c) When $\lambda > \lambda_h$, let $\lambda^c = \lambda_h$. The cable tensions can be written as

$$\boldsymbol{T} = \boldsymbol{T} + \lambda^c \cdot \boldsymbol{N}\left(\boldsymbol{J}^T\right) = \boldsymbol{T}_{\max}. \tag{16}$$

That is, the cable tension is larger than the maximum allowable tension force, and the cable tension will be corrected to the maximum tension force at this time.

3.2.2. Minimum 3-norm optimization algorithm

The minimum 3-norm optimization objective function $f(\lambda)$ of cable tensions can be expressed as

$$f(\lambda) = \min\left(\sqrt[3]{t_1^3 + t_2^3 + t_3^3 + t_4^3}\right). \tag{17}$$

Since $y = \sqrt[3]{x}$ is a monotonic function, so let:

$$\begin{cases} f = \left(t_1^3 + t_2^3 + t_3^3 + t_4^3\right) = \sum_{i=1}^{4} \left(t_{s,i} + n_i\lambda\right)^3 = A\lambda^3 + B\lambda^2 + C\lambda + D \\ A = n_1^3 + n_2^3 + n_3^3 + n_4^3 \\ B = 3\left(t_{s,1}n_1^2 + t_{s,2}n_2^2 + t_{s,3}n_3^2 + t_{s,4}n_4^2\right) \\ C = 3\left(t_{s,1}^2 n_1 + t_{s,2}^2 n_2 + t_{s,3}^2 n_3 + t_{s,4}^2 n_4\right) \\ D = t_{s,1}^3 + t_{s,2}^3 + t_{s,3}^3 + t_{s,4}^3 \end{cases}. \tag{18}$$

https://doi.org/10.1017/S0263574721000448 Published online by Cambridge University Press

There are two situations for the optimization objective function $f(\lambda)$:

(1) When $A \neq 0$, then f is a cubic function. There is $\frac{\partial f}{\partial \lambda} = 3A\lambda^2 + 2B\lambda + C$, let $\frac{\partial f}{\partial \lambda} = 0$, there are also two situations:
① When $B^2 - 3AC < 0$, the function f is a monotonic function. If $A>0$, the function f is a monotonically increasing function; if $A<0$, then the function f is a monotonically decreasing function. Therefore:

$$\begin{cases} \lambda^c = \lambda_l, & (A > 0) \\ \lambda^c = \lambda_h, & (A < 0) \end{cases}. \tag{19}$$

② When $B^2 - 3AC \geq 0$, the function f is not a monotonic function, which has the following two poles:

$$\begin{cases} \lambda_1 = \dfrac{-B - \sqrt{B^2 - 3AC}}{3A} \\ \lambda_2 = \dfrac{-B + \sqrt{B^2 - 3AC}}{3A} \end{cases}. \tag{20}$$

At this time, if $A > 0$ $\begin{cases} \lambda_1 < \lambda_2 < \lambda_l, & \lambda^c = \lambda_l \\ \lambda_1 < \lambda_l < \lambda_2, & \lambda^c = \lambda_2 \\ \lambda_l < \lambda_1 < \lambda_2 < \lambda_h, & f = \min(f_l, f_2) \\ \lambda_1 < \lambda_h < \lambda_2, & f = \min(f_l, f_h) \\ \lambda_h < \lambda_1 < \lambda_2, & \lambda^c = \lambda_l \end{cases}$; if $A < 0$, $\begin{cases} \lambda_2 < \lambda_1 < \lambda_l, & \lambda^c = \lambda_h \\ \lambda_2 < \lambda_l < \lambda_1, & f = \min(f_l, f_h) \\ \lambda_l < \lambda_2 < \lambda_1 < \lambda_h, & f = \min(f_2, f_h) \\ \lambda_2 < \lambda_h < \lambda_1, & \lambda^c = \lambda_2 \\ \lambda_h < \lambda_2 < \lambda_1, & \lambda^c = \lambda_h \end{cases}$.

(2) When $A = 0$, the function f is a quadratic function, and $B > 0$, $\frac{\partial f}{\partial \lambda} = 2B\lambda + C$. Let $\frac{\partial f}{\partial \lambda} = 0$, so:

$$\lambda = -\frac{C}{2B}. \tag{21}$$

Hence, there is $\begin{cases} \lambda < \lambda_l & \lambda^c = \lambda_l \\ \lambda_l < \lambda < \lambda_l & \lambda^c = \lambda_l \\ \lambda_h < \lambda & \lambda^c = \lambda_h \end{cases}$.

The cable tension optimized is $\boldsymbol{T} = \boldsymbol{J}^{+}\boldsymbol{F} + \lambda^c \cdot \boldsymbol{N}(\boldsymbol{J}^T)$ with the minimum 3-norm algorithm.

3.2.3. Minimum variance optimization algorithm

When the minimum variance of cable tensions is used as the optimization objective function, the distribution of cable tensions is more uniform, which helps to improve the stability of system movement and ensure the safety of patients in rehabilitation training. The optimization objective function $f(\lambda)$ of cable tensions can be expressed as

$$f(\lambda) = \frac{1}{4}\left[\sum_{i=1}^{4}(t_i - E(t))^2\right], \tag{22}$$

where $E(t) = \dfrac{t_1 + t_2 + t_3 + t_4}{4} = \dfrac{\sum_{i=1}^{4}(t_{s,i} + n_i\lambda)}{4}$ is the average value of cable tensions at the current moment. Let:

$$\begin{cases} f = \dfrac{1}{4}\left[\sum_{i=1}^{4}(t_i - E(t))^2\right] \\ L = t_{s,1} + t_{s,2} + t_{s,3} + t_{s,4}, & N = n_1 + n_2 + n_3 + n_4 \\ S = t_{s,1}^2 + t_{s,2}^2 + t_{s,3}^2 + t_{s,4}^2, & Q = n_1^2 + n_2^2 + n_3^2 + n_4^2 \end{cases}, \tag{23}$$

https://doi.org/10.1017/S0263574721000448 Published online by Cambridge University Press

f can be further organized as

$$f = \frac{1}{4}\left[\sum_{i=1}^{4}(t_i - E(t))^2\right] = A\lambda^2 + B\lambda + C, \tag{24}$$

where $A = \frac{Q}{4} - \frac{N^2}{16}$, $B = -\frac{LN}{8}$, $C = \frac{S}{4} - \frac{L^2}{16}$. Due to $A > 0$, So f has a minimum, and $\frac{\partial f}{\partial \lambda} = 2A\lambda + B$. Let $\frac{\partial f}{\partial \lambda} = 0$, $\lambda = -\frac{B}{2A}$. There are three situations at this time:

(a) When $\lambda_l \le \lambda \le \lambda_h$, $\lambda^c = \lambda$. The cable tensions can be written as

$$\boldsymbol{T} = \boldsymbol{T}_s + \lambda^c \cdot \boldsymbol{N}\left(\boldsymbol{J}^T\right). \tag{25}$$

(b) When $\lambda < \lambda_l$, let $\lambda^c = \lambda_l$. The cable tensions can be written as

$$\boldsymbol{T} = \boldsymbol{T}_s + \lambda^c \cdot \boldsymbol{N}\left(\boldsymbol{J}^T\right) = \boldsymbol{T}_{\min}. \tag{26}$$

That is, the cable tension is smaller than the minimum pre-tension force, and the cable tension will be corrected to the minimum cable tension at this time.

(c) When $\lambda > \lambda_h$, let $\lambda^c = \lambda_h$. The cable tensions can be written as

$$\boldsymbol{T} = \boldsymbol{T} + \lambda^c \cdot \boldsymbol{N}\left(\boldsymbol{J}^T\right) = \boldsymbol{T}_{\max}. \tag{27}$$

That is, the cable tension is larger than the maximum allowable tension force, and the cable tension will be corrected to the maximum tension force at this time.

3.2.4. CF optimization algorithm

In CF optimization algorithm, let:

$$\boldsymbol{T}_n = \frac{\boldsymbol{T}_{\min} + \boldsymbol{T}_{\max}}{2}. \tag{28}$$

The mechanical equilibrium Eq. (3) of the CDLR can be arranged as

$$\boldsymbol{J}^T(\boldsymbol{T}_s + \boldsymbol{T}_n) = \boldsymbol{F}. \tag{29}$$

Equation (29) can be transformed into as

$$\boldsymbol{J}^T\boldsymbol{T}_s = \boldsymbol{F} - \boldsymbol{J}^T\boldsymbol{T}_n. \tag{30}$$

Hence,

$$\boldsymbol{T}_s = \boldsymbol{J}^+\left(\boldsymbol{F} - \boldsymbol{J}^T\boldsymbol{T}_n\right). \tag{31}$$

Substitute Eq. (31) into Eq. (5), it can be obtained that the optimized cable tension is

$$\boldsymbol{T} = \boldsymbol{T}_n + \boldsymbol{J}^+\left(\boldsymbol{F} - \boldsymbol{J}^T\boldsymbol{T}_n\right). \tag{32}$$

It can be seen that the calculation process of the CF optimization algorithm is straightforward, so the real-time calculation is good, and the cable tensions calculated along the trajectory of the end effector are also continuous.

3.3. Feasible workspace

The feasible workspace of the CDLR refers to the set of reachable positions of the lower limb traction point under the premise of meeting the constraints of the CDLR system. Therefore, the feasible workspace W^c of the CDLR can be expressed as

$$W^c = \{(x, y, z) \mid g_0(x, y, z) \le 0\}, \tag{33}$$

where $g_0(x, y, z)$ is the constraints of the CDLR system.

https://doi.org/10.1017/S0263574721000448 Published online by Cambridge University Press

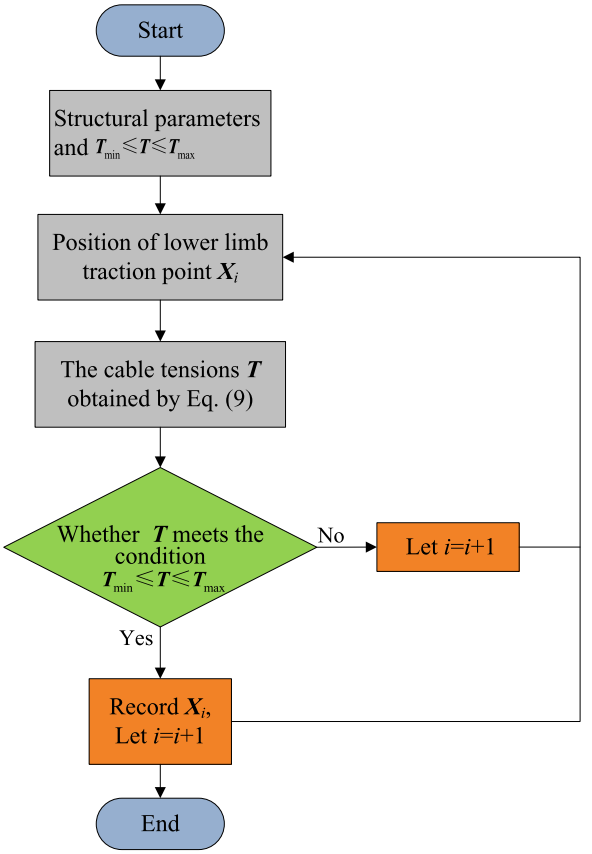


Figure 2. *Calculation flow chart of the feasible workspaces of the CDLR.*

In addition, the quality of the workspace is a good evaluation index of the motion performance of the robot system. Normally, the determinant of the structure matrix is used to define the quality of the robot's workspace, but the determinant of the matrix cannot well reflect the accuracy degree and stability of the system solution [36]. Therefore, this study will use the condition number of the structure matrix to measure the quality of the workspace for the CDLR, and the condition number of the structure matrix can well reflect the accuracy and stability of the system solution. The quality of the workspace for the CDLR can be expressed as

$$Q = \mathrm{cond}(\boldsymbol{J}^{+}) = \sigma_{\max} / \sigma_{\min}, \tag{34}$$

where $\sigma_{\max}$ and $\sigma_{\min}$ respectively represent the maximum singular value and the minimum singular value of the matrix J^{+}.

It can be seen from Eq. (34) that the value range of the quality of the workspace is $Q \in [1, 8\infty)$. When $Q = 1$, the motion transmission performance of the CDLR system is the best, which means that the quality of the workspace for the CDLR is the best; but when $Q \to \infty$, the lower limb traction point is in a singular position. At this time, the motion mechanics transmission performance of the CDLR system is very poor. Therefore, when designing a CDLR, the quality of the workspace should be as small as possible. In addition, the calculation flow chart of the feasible workspaces of the CDLR is shown in Fig. 2.

https://doi.org/10.1017/S0263574721000448 Published online by Cambridge University Press

4. Results and discussion

In order to analyze the real-time performance of the proposed optimization algorithms and the influence of the optimization algorithms on the mechanical characteristics of the CDLR, the cable tensions of the CDLR are calculated using MATLAB 2019b (64bit) on the computer that the CPU is AMD Athlon II X3 425 and memory is 8G DDR3 1333MHz. This study takes the motion trajectory of the normal walking gait in Clinical Gait Analysis (CGA) as the expected trajectory for analysis. The expected trajectory of the lower limb traction point can be written as

$$\begin{cases} x = x_{OP} \\ y = y_{OP} + a_1 \sin\theta_1 + a_2 \sin(\theta_1 + \theta_2) \\ z = z_{OP} - a_1 \cos\theta_1 - a_2 \cos(\theta_1 + \theta_2) \\ \theta_1 = 20 \sin(\omega t) + 10 \\ \theta_2 = 30 \cos(\omega t) - 30 \end{cases}, \tag{35}$$

where (x_{OP}, y_{OP}, z_{OP}) is the position of the hip. a_1 and a_2 denote the length of the thigh and calf of the lower limb, respectively. θ_1 and θ_2 denote the angular displacement of the hip and knee joints, respectively. ω is a variable that is related to the exercise ability of trained objects.

A real-time performance evaluation index is given to measure the calculation speed of the above-mentioned optimization algorithms:

$$t_{\text{mean}} = \frac{\sum_{i=1}^{N} t(\boldsymbol{X}_i)}{N}, \tag{36}$$

where t_{mean} is real-time performance evaluation index of the optimization algorithm, which indicates the average value of the time required to calculate the cable tensions. $t(X_i)$ indicates the time required to calculate the cable tensions at the location point X_i. N is the number of calculation location points.

The structural parameters of the designed CDLR are as follows: pulleys position b_1=[500, 0, 800]^{T}mm, b_2=[0, 0, 800]^T mm, $b_3 = [0, 1680, 800]^T$ mm, and $b_4 = [500, 1680, 800]^T$ mm.10 N $\leq \boldsymbol{T} \leq$ 500 N. The force of the lower limbs on the traction point as a constant force in the vertical direction, $\boldsymbol{F}$ = [0, 0, -98] N.

The feasible workspaces of the CDLR calculated by different optimization algorithms are shown in Fig. 3(a)-(d). The calculation step length under the minimum 2-norm optimization algorithm, minimum 3-norm optimization algorithm, minimum variance optimization algorithm, and CF optimization algorithm is the same. The performances of the feasible workspace for the CDLR obtained by different optimization algorithms are shown in Table 1.

It can be seen from Fig. 3(a)-(c) and Table 1 that when the minimum 2-norm, minimum 3-norm, and minimum variance optimization algorithms are used as the optimization objective function, the volume sizes of the feasible workspace of the CDLR are basically the same, but the minimum 3-norm optimization algorithm is used as the optimization objective function to calculate the feasible workspace, the time consumed is approximately 3.53 times and 3.55 times of the minimum 2-norm optimization algorithm and the minimum variance optimization algorithm. It shows that the real-time performance of the minimum 3-norm optimization algorithm is poorer than that of other optimization algorithms. In addition, Fig. 3(d) shows that the volume size of the feasible workspace for the CDLR obtained by the CF optimization algorithm is significantly smaller than that of the other three optimization algorithms, especially the lower and boundary areas of the feasible workspace. When the lower limb traction point is at the lower and boundary areas of the workspace, the cable tensions are seriously unevenly distributed, the pseudo-drag phenomenon of the cables may even occur. The CF optimization algorithm does not have a large correction ability of the cable tensions, and it only records the position points that meet the constraint conditions. However, using the CF optimization algorithm to calculate the feasible

https://doi.org/10.1017/S0263574721000448 Published online by Cambridge University Press

Table 1. *Performance of feasible workspace of the CDLR obtained by different optimization algorithms.*

Optimization algorithms	Total number of position points	t_{mean}/s	max(λ^c)	$\sigma_{\min}$	$\sigma_{\max}$	[min(Q), max(Q)]
2-Norm	104,001	2.6538×10^{-3}	2.4869×10^{-14}	0.1215	1.9131	[1.4028, 15.7067]
3-Norm	102,974	9.4490×10^{-3}	2.2501	0.1215	1.9131	[1.4028, 15.7067]
Minimum variance	104,001	2.6346×10^{-3}	1.6104×10^{-14}	0.1215	1.9131	[1.4028, 15.7067]
CF	86,572	2.5993×10^{-3}	/	0.1215	1.9131	[1.4150, 15.7067]

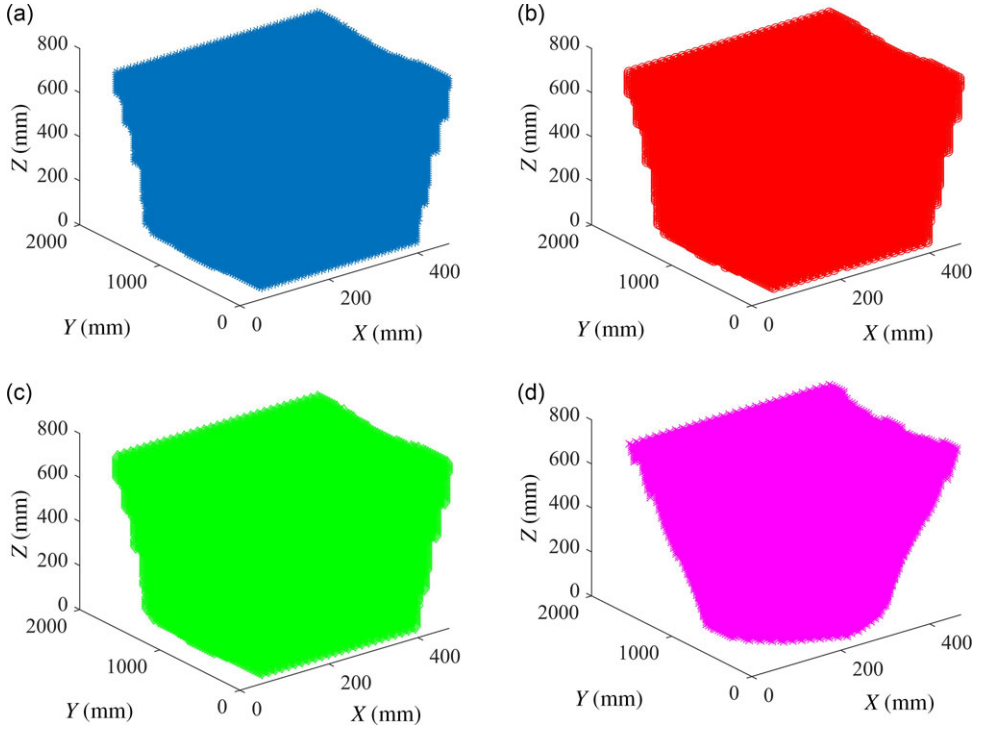


Figure 3. *Feasible workspaces of the CDLR obtained by different optimization algorithms. (a) Minimum 2-norm. (b) Minimum 3-norm. (c) Minimum variance. (d) CF.*

workspace of the CDLR, the consumed time is smallest, which indicates that the CF optimization algorithm has good real-time performance. Compared with the other three optimization algorithms, the CF optimization algorithm has a poorer ability to correct cable tension, but this will not affect the training performance of the CDLR, because the lower limb rehabilitation training tasks should be planned in the middle area of the workspace in general [21], which has practical significance for the safety of the trained object and the stability of the system.

Assuming that the position of the hip joint is fixed, and $(x_{OP}, y_{OP}, z_{OP}) = (250, 840, 800)$ mm. The length of the thigh and calf are 423.27 and 396.81 mm, respectively. At this time, the trajectory of the lower limb traction point is shown in Fig. 4. The change curves of cable tensions calculated by different optimization algorithms are shown in Fig. 5.

https://doi.org/10.1017/S0263574721000448 Published online by Cambridge University Press

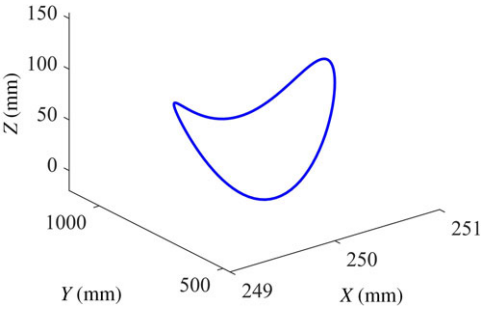


Figure 4. *Trajectory of the lower limb traction point.*

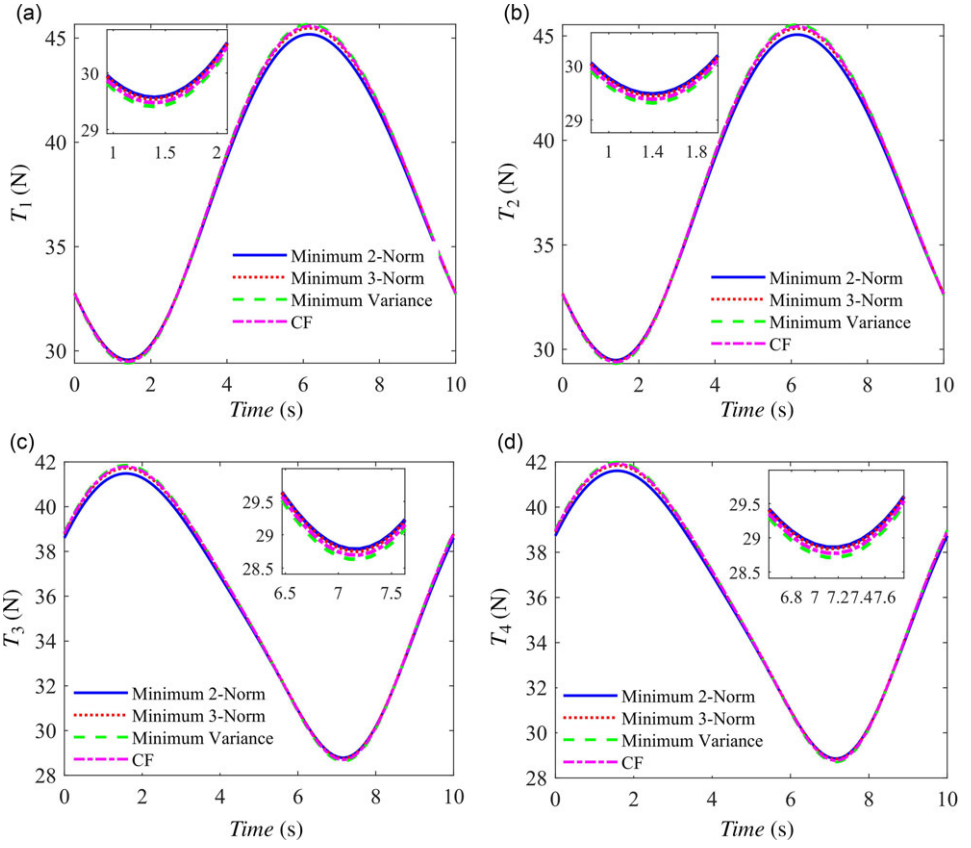


Figure 5. *Change curves of cable tensions calculated by different optimization algorithms. (a) Change curve of T_1. (b) Change curve of T_2·(c) Change curve of T_3. (d) Change curve of T_4.*

It can be seen from Fig. 5(a)-(d) that when different optimization algorithms are used as optimization objective function, the changes of the cable tensions are smooth and continuous, and the values of the cable tensions are basically the same. Since the trajectory of the lower limb traction point is in the section X = 250 mm, the cable tension changes of cable 1 and cable 2 are the same, and cable tension changes of cable 3 and cable 4 are the same. In addition, the cable tensions calculated by the minimum 2-norm optimization algorithm are relatively smaller overall, which is not good for enhancing and adjusting the system stiffness of the CDLR with low stiffness. The cable tensions calculated by the minimum variance

https://doi.org/10.1017/S0263574721000448 Published online by Cambridge University Press

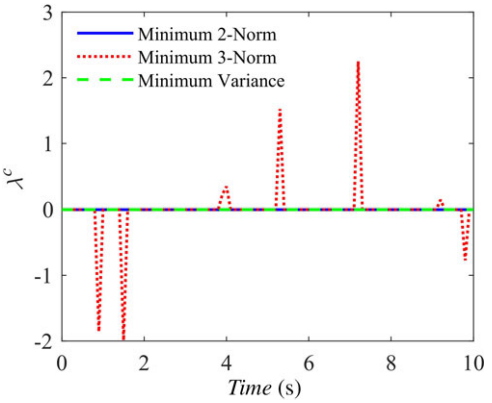


Figure 6. *Change curves of* λ^c.

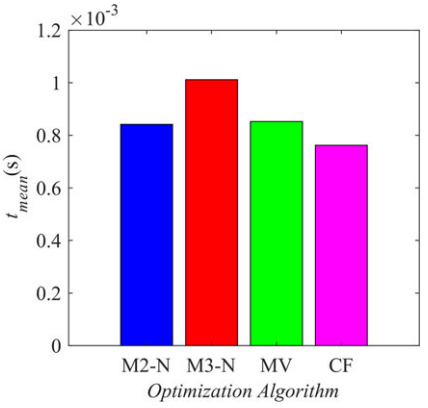


Figure 7. *Change curves of* t_{mean}.

optimization algorithm are greater than the cable tensions obtained by the minimum 3-norm optimization algorithm at the peaks and valleys. The cable tensions calculated by the CF optimization algorithm are between the cable tensions calculated by the minimum 3-norm optimization algorithm and the minimum variance optimization algorithm. Therefore, the minimum variance optimization algorithm has practical significance for improving the system stiffness of the CDLR.

When using the minimum 2-norm, minimum 3-norm, and minimum variance optimization algorithm to calculate the cable tensions, the change curves of the adjustment parameter λ^c are shown in Fig. 6. One can see that the change and volatility of the adjustment parameter λ^c with the minimum 2-norm and minimum variance optimization algorithms are small, but the change and volatility of the adjustment parameter λ^c with the minimum 3-norm optimization algorithms are larger, especially at the peak and trough of the cable tensions curves. It will cause obvious fluctuations of the change and distribution of the cable tensions, which have a negative effect on the safety of the trained object and the stability of the system.

The real-time evaluation index t_{mean} of cable tensions calculation with different optimization algorithms is shown in Fig. 7. The real-time evaluation index t_{mean} of the minimum 2-norm, minimum 3-norm, and minimum variance optimization algorithms are respectively 0.8416×10^{-3}, 1.0112×10^{-3}, 0.8525×10^{-3}, and 0.7624×10^{-3} s, which indicate that the minimum 3-norm optimization algorithm has the worst real-time performance, and the real-time performance of the minimum 2-norm and the minimum variance optimization algorithms is almost the same, and the CF optimization algorithm has the best real-time performance.

https://doi.org/10.1017/S0263574721000448 Published online by Cambridge University Press

It can be seen from the above analysis that the cable tensions value calculated by the minimum 2-norm optimization algorithm is relatively smaller overall. When the lower limb traction point is at the position where the cable tension is smaller, this may cause the vibration of the lower limb traction point. The correction ability of the cable tensions with the minimum 3-norm optimization algorithm is the strongest, but the volatility of the corrected cable tension is also more obvious, which is not good for the safety of trained patients. The calculation real-time performance of the CF optimization algorithm is the best, but the correction ability of the cable tension is poorer, and the obtained effective workspace is smaller. The distribution of the cable tensions calculated by the minimum variance optimization algorithm is more uniform, and the ability of the real-time calculation performance is better. Therefore, considering from the aspects of improving the active adjustment ability of the system stiffness for the CDLR, the stability and real-time performance of the system, and the safety of the trained object, the minimum variance optimization algorithm is more suitable for the optimization objective function of the cable tensions for the CDLR.

5. Conclusion

Aiming at the needs of lower limb rehabilitation training, a CDLR was designed and its mechanical characteristics were studied. The four kinds of optimization algorithms of the cable tensions were analyzed. The following conclusions were obtained:

(1) When the minimum 2-norm, minimum 3-norm, and minimum variance optimization algorithms are used as the optimization objective function of the cable tensions, the volume sizes of the feasible workspace for the CDLR are basically the same. The volume of feasible workspace for the CDLR obtained by the CF optimization algorithm is significantly smaller than that of the other three optimization algorithms, especially the lower and boundary areas of the feasible workspace. The qualities of the feasible workspace for the CDLR calculated by the four optimization algorithms are basically the same.

(2) The cable tensions value calculated by the minimum 2-norm optimization algorithm is relatively smaller overall. When the lower limb traction point is at the position where the cable tension is smaller, this may cause the vibration of the lower limb traction point. The correction ability of cable tensions with the minimum 3-norm optimization algorithm is the strongest, but the volatility of the corrected cable tension is also more obvious, which is not good for the safety of trained patients. The calculation real-time performance of the CF optimization algorithm is the best, but the correction ability of the cable tension is poorer, and the obtained effective workspace is smaller. The distribution of the cable tensions calculated by the minimum variance optimization algorithm is more uniform, and the ability of the real-time calculation is better.

(3) Since the acceptable exercise range of the lower limbs of patients with severe diseases or exercise disorders is small, the CF optimization algorithm and minimum variance optimization algorithm are more suitable for patients with severe diseases or movement disorders in the initial stage of rehabilitation training. When the patient recovers part of the exercise ability after a period of rehabilitation training, the training intensity needs to be appropriately increased to improve the effect of the patient's rehabilitation training. The minimum 2-norm optimization algorithm, the minimum 3-norm optimization algorithm, and minimum variance optimization algorithm have a certain correction ability of the cable tensions. Therefore, the minimum 2-norm optimization algorithm, the minimum 3-norm optimization algorithm, and minimum variance optimization algorithm are more suitable for the comprehensive training mode of patients in the later stage of rehabilitation training. Based on the above discussion, it can be seen that the minimum variance optimization algorithm is an optimization algorithm suitable for patients training in the entire rehabilitation phase.

Future work: the safety evaluation system of the CDLR and man-machine interaction compliance control strategy of the CDLR need to be further researched based on the results of this paper.

https://doi.org/10.1017/S0263574721000448 Published online by Cambridge University Press

Acknowledgments. This research is supported by the National Natural Science Foundation of China (61773007), Natural Science Foundation of Heilongjiang Province, China (LH2019E032), and the Fundamental Research Funds for Central Universities of the Harbin Engineering University (3072020CF0706).

References

[1] United Nations, "2019 Revision of World Population Prospects," New York , USA, 2019.
[2] Y. L. Wang, K. Y. Wang, W. Y. Zhao, W. L. Wang, Z. Han and Z. X. Zhang, "Effects of single crouch walking gaits on fatigue damages of lower extremity main muscles," *J Mech. Med. Biol.* **19**(6), 1940046 (2019).
[3] R. De-La-torre, E. D. Oña, C. Balaguer and A. Jardón, "Robot-aided systems for improving the assessment of upper limb spasticity: A systematic review," *Sensors* **20**(18), 5251 (2020).
[4] A. Basteris, S. M. Nijenhuis, A. H. A. Stienen, J. H. Buurke, G. B. Prange and F. Amirabdollahian, "Training modalities in robot-mediated upper limb rehabilitation in stroke: A framework for classification based on a systematic review," *J. NeuroEng. Rehabil.* **11,** 111–126 (2014).
[5] Y. L. Wang, K.Y. Wang and Z. X. Zhang, "Design, comprehensive evaluation, and experimental study of a cable-driven parallel robot for lower limb rehabilitation," *J. Braz. Soc. Mech. Sci. Eng.* **42**(7), 371, 1–21 (2020).
[6] Y. L. Wang, K. Y. Wang, Z. X. Zhang, Z. Han and Z. X. Zhang, "Appraisement and analysis of dynamical stability of under-constrained cable-driven lower limb rehabilitation training robot," *Robotica*, 1–14 (2020), published online. doi:10.1017/S0263574720000879.
[7] E. Sánchez, "Lower-limb robotic rehabilitation: Literature review and challenges," *J. Robot*. **11**, 759764, 1–11 (2011).
[8] X. Cui, W. H. Chen, X. Jin and K. A. Sunil, "Design of a 7-DOF cable-driven arm exoskeleton (CAREX-7) and a controller for dexterous motion training or assistance" *IEEE/ASME Trans. Mech.* **22**(1), 161–172 (2017).
[9] N. Aliman, R. Ramli and S. M. Haris, "Design and development of lower limb exoskeleton: A survey" *Rob. Auton. Syst.* **95**, 102–116 (2017).
[10] M. S. Amiri, R. Ramli, M. A. A. Tarmizi, A. Tarmizi and D. Narooei, "Simulation and control of a six degree of freedom lower limb exoskeleton" *J. Kejuruteraan* **32**(2), 197–204 (2020).
[11] A. L. Armannsdottir, P. Beckerle, J. C. Moreno, E. H. F. V. Asseldonk, M. T. Manrique-Sancho, A. J. Del-Ama, J. F. Veneman and K. Briem, "Assessing the involvement of users during development of lower limb wearable robotic exoskeletons: A survey study" *Hum. Factors* **62**(3), 351–364 (2020).
[12] Q. C. Wu, X. S. Wang and F. P. Du, "Analytical inverse kinematic resolution of a redundant exoskeleton for upper-limb rehabilitation" *Int. J. Hum. Rob.* **13**(3), 1550042 (2016).
[13] Q. C. Wu, X. S. Wang, H. T. Wu and B. Chen, "Fuzzy sliding mode admittance control of the upper limb rehabilitation exoskeleton robot," *Robot* **40**(4), 457–465 (2018).
[14] S. Qian, B. Zi, W.-W. Shang and Q. S. Xu, "A review on cable-driven parallel robots" *Chin. J. Mech. Eng*. **31**(4), 66–77 (2018).
[15] B. Zi, G. C. Yin, Y. Li and D. Zhang, "Kinematic Performance Analysis of a Hybrid-Driven Waist Rehabilitation Robot," *2nd International Conference on Mechatronics and Robotics Engineering (ICMRE)*, Nice, France (2016).
[16] Q. Chen, B. Zi, Z. Sun, Y. Li and Q. S. Xu, "Design and development of a new cable-driven parallel robot for waist rehabilitation" *IEEE-ASME Trans. Mech*. **24**(4), 1497–1507 (2019).
[17] D. Cafolla, M. Russo and G. Carbone, "CUBE, a cable-driven device for limb rehabilitation" *J. Bionic. Eng.* **16**(3), 492–502 (2019).
[18] A. M. Barbosa, J. C. M. Carvalho and R. Gonçalves, "Cable-driven lower limb rehabilitation robot," *J. Braz. Soc. Mech. Sci. Eng.* **40**(5), 345, 1–11 (2018).
[19] Y. L. Wang, K. Y. Wang, Z. Zhang, Z. Han and W. L. Wang, "Analysis of dynamical stability of rigid-flexible hybrid-driven lower limb rehabilitation robot," *J. Mech. Sci. Tech.* **34**(4), 1735–1748 (2020).
[20] K.-Y. Wang, P.-C. Yin, H.-P. Yang and X. Q. Tang, "The man-machine motion planning of rigid-flexible hybrid lower limb rehabilitation robot," *Adv. Mech. Eng*. **10**(6), 1–11 (2018).
[21] Y. L. Wang, K. Y. Wang, W. L. Wang, P. C. Yin and Z. Han, "Appraise and analysis of dynamical stability of cable-driven lower limb rehabilitation training robot" *J. Mech. Sci. Tech.* **33**(11), 5461–5472 (2019).
[22] Y. Wang, K. Wang, W. Wang, Z. Han and Z. Zhang, "Appraisement and analysis of dynamical stability of under-constrained cable-driven lower-limb rehabilitation training robot" *Robotica*, 1–14 (2020). published online. doi:10.1017/S0263574720000879.
[23] Y. L. Wang, K. Y. Wang, K. C. Wang and Z. J. Mo, "Safety evaluation and experimental study of a new bionic muscle cable-driven lower limb rehabilitation robot" *Sensors* **20**(24), 7020 (2020).
[24] I. B. Hamida, M. A. Laribi, A. Mlika, L. Romdhane, S. Zeghloul and G. Carbone, "Multi-objective optimal design of a cable driven parallel robot for rehabilitation tasks," *Mech. Mach. Theory* **156**, 104141 (2021).
[25] Y. Su, Y. Y. Qiu and H. L. Wei, "Dynamic modeling and tension optimal distribution of cable-driven parallel robots considering cable mass and inertia force effects," *Eng. Mech.* **33**(11), 231–239 + 248 (2016).

https://doi.org/10.1017/S0263574721000448 Published online by Cambridge University Press

[26] X. Q. Tang, X. M. Chai, L. W. Tang and Z. F. Shao, "Accuracy synthesis of a multi-level hybrid positioning mechanism for the feed support system in FAST" *Rob. Comput. Integr. Manuf.* **30**(5), 565–575 (2014).
[27] F. Zhang, B. Zhang, F. Zhou, W. W. Shang and S. Cong, "Configuration selection and parameter optimization of redundantly actuated cable-driven parallel robots," *J. Mech. Eng.* **56**(1), 1–8 (2020).
[28] Y. L. Wang, K. Y. Wang, Z. X. Zhang and Z. J. Mo, "Control strategy and experimental research of a cable-driven lower limb rehabilitation robot," *Proc. Inst. Mech. Eng. Part C-J. Eng. Mech. Eng. Sci*., 1–14 (2020), published online, doi:10.1177/0954406220952510.
[29] Y. L. Wang, K. Y. Wang, Z. X. Zhang, L. L. Chen and Z. J. Mo, "Mechanical characteristics analysis of a bionic muscle cable-driven lower limb rehabilitation robot," *J. Mech. Med. Biol.* **20**(10), 2040037 (2020).
[30] G. Boschetti and A. Trevisani, "Cable robot performance evaluation by Wrench exertion capability," *Robotics* **7**(2), 15 (2018).
[31] S. Zhang, D. X. Cao, H. Min, S. Li and X. L. Zhang, "Design and wrench-feasible workspace analysis of a cable-driven hybrid joint," *Int. J. Adv. Rob. Syst.* **17**(1), 1729881419899758 (2020).
[32] H. Wang, W. Li, H. Liu, J. Zhang and S. Liu, "Conceptual design and dimensional synthesis of a novel parallel mechanism for lower-limb rehabilitation," *Robotica* **37**(3), 469–480 (2019).
[33] A. Aflakian, A. Safaryazdi, M. T. Masouleh and A. Kalhor, "Experimental study on the kinematic control of a cable suspended parallel robot for object tracking purpose," *Mechatronics* **50**, 160–176 (2018).
[34] Y. Zou, N. Wang, K. Liu and X. Geng, "Design and analysis of movable cable-driven lower limb rehabilitation robot," *J. Huazhong Univ. Sci. Tech.* (*Natural Science Edition*) **47**(1), 22–26 and 38 (2019).
[35] Y. Su, "Mechanical analysis and performance optimization of wire driven parallel robot," Xi'dian University (2014).
[36] Z. G. Zhao, Y. L. Wang, Y. Ma, C. Su, J. S. Li and G. Ji, "Dynamical workspace of multi-robot collaborative towing system," *J. Harbin Eng. Univ*. **38**(7), 1079–1085+1161 (2017).

Cite this article: Y.-l. Wang, K.-y. Wang , Y.-j. Chai, Z.-j. Mo and K.-c. Wang (2022). "Research on mechanical optimization methods of cable-driven lower limb rehabilitation robot", Robotica **40**, 154–169. https://doi.org/10.1017/S0263574721000448

https://doi.org/10.1017/S0263574721000448 Published online by Cambridge University Press